Non-classical critical precipitates in a nucleation and growth regime: Reconciliation of simulation and experiment

L. Lunéville, P. Garcia, O. Tissot, David Simeone

Applied Physics Letters

Non-classical critical precipitates in a nucleation and growth regime: Reconciliation of simulation and experiment

Cite as: Appl. Phys. Lett. **121**, 184102 (2022); https://doi.org/10.1063/5.0122126
Submitted: 22 August 2022 • Accepted: 19 October 2022 • Published Online: 03 November 2022

L. Lunéville, P. Garcia, O. Tissot, et al.

Applied Physics Letters ARTICLE scitation.org/journal/apl

Non-classical critical precipitates in a nucleation and growth regime: Reconciliation of simulation and experiment

Cite as: Appl. Phys. Lett. **121**, 184102 (2022); doi: 10.1063/5.0122126
Submitted: 22 August 2022 · Accepted: 19 October 2022 ·
Published Online: 3 November 2022

L. Lunéville,[1] P. Garcia,[2] O. Tissot,[3] and D. Simeone[3,a)]

AFFILIATIONS

[1]Université Paris-Saclay, CEA, DES-Service de Recherche en Mathématiques Appliquées, 91191 Gif-sur-Yvette, France
[2]CEA, DES, DEC, Centre de Cadarache, 13108 Saint-Paul-Lez-Durance Cedex, France
[3]Université Paris-Saclay, CEA, DES-Service de Recherche Métallurgie Appliquée, 91191 Gif-sur-Yvette, France

[a)]Author to whom correspondence should be addressed: david.simeone@cea.fr

ABSTRACT

In this study, we have derived a method which consists in setting up and solving an original dynamics that provides critical precipitate characteristics, thus circumventing the theoretical difficulties encountered when modeling nucleation phenomena. Our model constitutes a substantial advance in this field as it enables critical nuclei characteristics to be determined irrespective of the energy barriers associated with the metastable state. Furthermore, the method is entirely consistent with the phase field approach, and in that respect, can be viewed as extending its applicability beyond the coarsening stage alone. The theoretical and numerical developments presented are assessed against original data obtained on an Fe-Cr alloy, used as a model system for studying nucleation and growth in the context of first order phase transitions.

Nucleation and growth processes are important to understanding many physical and biological phenomena ranging from crystallization, melting, and evaporation to the formation of clouds and neurodegenerative diseases.[1–4] Modeling critical precipitates involved in nucleation and growth processes constitutes a major challenge with substantial implications in these diverse fields,[5–9] since the morphology and concentration of critical precipitates control the long-term evolution of the physical system. The formation of the new phase from the parent one falls in two distinct categories, depending upon the energy barriers involved in the nucleation process. In the spinodal decomposition regime, there are no energy barriers to be overcome for precipitates to form and the decomposition kinetics may be modeled using the Cahn–Hilliard (CH) equation.[10] In the nucleation and growth regime, finite energy barriers exist, and a large number of computational methods have been used to investigate critical precipitates. However, most methods fail to reproduce the characteristics of nuclei experimentally observed. This precludes a quantitative or even a qualitative description of late-stage microstructures.

Indeed, numerous studies based on Becker and Doring's work have attempted to compute these critical precipitate characteristics[11,12] and have led to what is known as Classical Nucleation Theory (CNT). In CNT, each critical precipitate exhibits a uniform composition equal to the equilibrium composition of the bulk of the new phase. The width of the interfacial layer between the precipitate and matrix is assumed infinitely small and the critical precipitate is defined by its radius only. Although CNT has been successfully used to describe liquid–vapor transitions,[13–15] in solid–solid nucleation processes, for instance, critical precipitates are shown to exhibit a concentration at their core, which is different from that expected from the equilibrium phase diagram,[16] thus casting doubt upon the applicability of CNT in a more general context.

Cahn and Hilliard[10,17] first proposed the phase-field approach as an alternative to CNT in order to provide an improved description of the composition of critical precipitates. In this method, one assumes that the free energy is a functional of the local composition $c(\mathbf{x})$ by adding a Ginzburg term to the homogeneous free energy density. Critical precipitates correspond to saddle points of this functional, which could, in principle, be computed directly. However, this is an arduous task since the functional is highly non-linear. Alternatives must, therefore, be sought.

One such alternative has been proposed,[18,19] which involves adding random Langevin forces to the CH equation, thus forcing the

system to cross the energy barrier and to escape the local minimum the metastable state constitutes. This stochastic phase-field approach provides a realistic description of critical precipitates when the energy barrier is small, i.e., near the spinodal line.[20] However, to generate these precipitates using Langevin forces when the energy barrier is large, introduction of noise with unrealistically large amplitude is required. As the critical nucleus concentration is dependent upon the amplitude of noise, this, in turn, may lead to erroneous particle densities.[21]

In this Letter, we present an original method for modeling critical precipitates within a phase-field framework, which circumvents a detailed description of the nucleation process. This is done by calculating critical precipitate characteristics directly, from the knowledge of the free energy associated with the phase transition. The only assumption made is that critical precipitates correspond to an index-1 saddle point in the free energy landscape.[16] Our approach is of very general applicability and, therefore, may be used in many different physics and chemistry problems since no assumptions are made in regard to the interface layer thickness, the height of the energy barrier, or the degree to which the free energy is isotropic. We use the paradigm of the phase decomposition in immiscible binary alloys to demonstrate the relevance of our method.

For an $A_{1-\bar{c}}B_{\bar{c}}$ alloy, minima, maxima, and saddle points may be obtained from finding local extrema of the free energy under some species' conservation constraint ($\int[c(\mathbf{x})-\bar{c}]d\mathbf{x}=0$). Constrained optimization may be implemented using the Lagrangian multiplier μ, and setting to zero, the first variation of the Grand potential functional $\Omega[c(\mathbf{x})]$, which is given by

$$\Omega[c]=\int\left[\frac{\kappa}{2}|\nabla c(\mathbf{x})|^2+f(c(\mathbf{x}))-f(\bar{c})-\mu(c(\mathbf{x})-\bar{c})\right]d\mathbf{x}. \quad (1)$$

The first term in this expression is the Ginzburg term which accounts for the presence of a heterogeneous concentration field $c(\mathbf{x})$. κ is a phenomenological positive coefficient which represents the energetic cost associated with the formation of a spatial heterogeneity. Its value is assumed independent of $c(\mathbf{x})$ in the following. The homogeneous free energy density of the system is given by the functional $f(c(\mathbf{x}))$. $\mu=\frac{df}{dc}(\bar{c})$ is determined by setting $\frac{\delta\Omega[c]}{\delta c}$ to zero and further noticing that far from the precipitate, $c=\bar{c}$.[16,17] Note that although the gradient-dynamics ($\frac{\partial c(\mathbf{x},t)}{\partial t}\propto-\frac{\partial\Omega}{\partial c(\mathbf{x},t)}$) which models the time evolution of $c(\mathbf{x},t)$ differs from that derived from the CH equation ($\frac{\partial c(\mathbf{x},t)}{\partial t}\propto\Delta\frac{\partial\Omega}{\partial c(\mathbf{x},t)}$), the stationary points of both dynamics are identical.[22] In other words, once critical precipitates are determined from the identification of the saddle points of $\Omega[c(\mathbf{x})]$, the CH equation can take over to model the growth kinetics of precipitates.

Setting to zero, the first variation of $\Omega[c(\mathbf{x})]$ [Eq. (1)] with respect to c yields the concentration profile $c(\mathbf{x})$ around the critical precipitates and leads to the following, second order, partial differential equation:

$$-\kappa\Delta c+\frac{df(c)}{dc}=\frac{df(\bar{c})}{dc}. \quad (2)$$

Assuming that there is no flux of matter or chemical potential at the surface of the integration domain, one may derive the boundary conditions associated with Eq. (2), which are given by $\nabla c=0$ and $\nabla^3 c=0$.

Solving Eq. (2) yields all stationary solutions, i.e., maxima, minima, and saddle points. It is, therefore, necessary to calculate $\frac{\delta^2\Omega[c]}{\delta c^2}$ at each spatial discretization point, the second variation of $\Omega[c]$ with respect to $c(\mathbf{x})$, in order to differentiate saddle points from other extrema. Equation (2) cannot be solved analytically and the numerical determination of $\frac{\delta^2\Omega[c]}{\delta c^2}$ requires extensive computational resources. An alternative solution consists in setting up a fictitious dynamics, the stationary solution to which necessarily corresponds to the desired saddle point. The Constrained Shrinking Dimer Dynamics (CSDD)[23] or its extension, the Gentlest Ascent Dynamics (GAD),[24] are examples of such a strategy. Assuming that the index of the saddle point of $\Omega[c]$ is one, i.e., $\frac{\delta^2\Omega[c]}{\delta c^2}$ exhibits a unique negative eigenvalue at the saddle point, the GAD dynamics may be written as

$$\frac{\partial c}{\partial t}=-\frac{\delta\Omega[c]}{\delta c}+2\left\langle\frac{\delta\Omega[c]}{\delta c}\middle|v\right\rangle v, \quad (3a)$$

$$\frac{\partial v}{\partial t}=-\frac{\delta^2\Omega[c]}{\delta c^2}v+\left\langle v\middle|\frac{\delta^2\Omega[c]}{\delta c^2}\middle|v\right\rangle v, \quad (3b)$$

where the term $\langle\cdot|\cdot\rangle$ refers to the scalar product of $L^2(\mathbb{R}^3)$. Equation (3a) is a gradient dynamics to which an "ascent" force is added, thus enabling $c(\mathbf{x},t)$ to escape the metastable phase resulting from the high temperature quench. The normalized vector v that appears in Eq. (3a) defines the "ascent" direction and converges toward an eigenvector of $\frac{\delta^2\Omega[c]}{\delta c^2}$.[24]

This dynamics suffers from a number of shortcomings. If the initial condition $c(\mathbf{x},0)$ is far removed from the concentration profile at the saddle point, it does not converge.[25,26] When it does converge, the convergence is slow.[27] If the initial condition for $v(\mathbf{x},0)$ is randomly chosen, trajectories generated by Eq. (3b) will not escape the metastable state.

To overcome these difficulties, we have implemented a modified GAD dynamics in which vector $v(\mathbf{x},t)$ (hereafter noted $v_0(\mathbf{x})$) no longer results from solving Eq. (3b) but is time-independent and equal to the most unstable direction of $\Omega[c]$. This vector is always the eigenvector associated with the smallest eigenvalue of $\frac{\delta^2\Omega[c]}{\delta c^2}$ determined using the conjugate gradient algorithm. The proposed dynamics may now be expressed as

$$\frac{\partial c}{\partial t}=-\frac{\delta\Omega[c]}{\delta c}+2\left\langle\frac{\delta\Omega[c]}{\delta c}\middle|v_0\right\rangle v_0. \quad (4)$$

As a result of this choice for $v_0(\mathbf{x})$, Eq. (4) converges systematically and its initial condition may be chosen as the homogeneous concentration profile $\bar{c}$ determined by the high temperature phase. Choosing an initial value for $c(x,0)$ is no longer an issue. These two aspects of our method make it substantially different from the CCSD or GAD methods.

Assuming $c(\mathbf{x},t)$ and $v_0(\mathbf{x})$ are periodic, the boundary conditions ($\nabla c(\mathbf{x},t)=\nabla v_0(\mathbf{x})=0$ and $\nabla^3 c(\mathbf{x},t)=\nabla^3 v_0(\mathbf{x})=0$) suggest expanding these functions as cosine transforms.[28] A first order Euler scheme is used for solving Eq. (4). As $f(c)$ is a highly non-linear function of $c(\mathbf{x},t)$, Eyre's approach[29,30] is applied providing an unconditionally gradient stable scheme and enabling large time step values to be chosen. The steady state solution to Eq. (4), i.e., the concentration profile around critical precipitates, is obtained when $||\frac{\delta\Omega[c]}{\delta c}||_{L^2}\leq\varepsilon$ and $|\frac{\partial c}{\partial t}|\leq\varepsilon$, where $\varepsilon=10^{-5}$ is the chosen tolerance.

We now apply these developments to the demixion observed at low temperature in $Fe_{1-\bar{c}}Cr_{\bar{c}}$ alloys. The metastable high temperature homogeneous solid solution decomposes into Cr-rich precipitates in a Fe-rich matrix for $\bar{c} < \frac{1}{2}$ below $T_0 = 1000\,K$. Since the misfit between the Fe and Cr unit cells is small (<0.3%), the contribution to $\Omega[c]$ of the elastic energy resulting from the formation of Cr-rich coherent precipitates can be neglected and the Landau expansion of $f(c)$ is simply given by $f(c) = \frac{a_2(c(\mathbf{x},t)-c_0)^2}{2} + \frac{a_4(c(\mathbf{x},t)-c_0)^4}{4} + \frac{a_6(c(\mathbf{x},t)-c_0)^6}{6}$.[31] The coefficients that appear in this expression are determined at 773 K from our knowledge of the phase diagram:[32–34] $a_2 = -0.64\,\mathrm{eV/nm^3}$, $a_4 = -920\,\mathrm{eV/nm^3}$ are both negative and $a_6 = 7480\,\mathrm{eV/nm^3}$ is positive as expected from Landau theory of first order phase transitions.[31] The solubility limits for the Fe-rich matrix, the Cr-rich precipitates, and the spinodal line are equal to $c_\alpha = 0.147$, $c_\beta = 0.857$, and $c_s = 0.228$, respectively. Moreover, $\kappa = 6.1\,\mathrm{eV/nm}$[16] is derived from Monte Carlo surface free energy simulations performed at $T = 773\,\mathrm{K}$.[35] A possible concentration dependence of κ can be introduced as proposed by Cahn,[17] this concentration dependence does not modify the modified GAD method we propose but may lead to numerical instabilities for algorithms. For the FeCr alloys, previous investigations[35,36] clearly show that κ has no concentration dependence.

All simulations were performed with a dimensionless time step of 0.01. The dimensionless 3D mesh size, Δx, was chosen equal to 0.1, ensuring that the interface is correctly described. The dimension of the integration volume ($V = 32\Delta x \times 32\Delta x \times 32\Delta x$) is large enough to guarantee the conservation of species, i.e., $\frac{1}{V}\left|\int (c(\mathbf{x},t) - \bar{c})d\mathbf{x}\right| < 10^{-3}$.

Figure 1 shows the steady-state solution of Eq. (4), $c(\mathbf{x})$, across a critical precipitate (magenta line) obtained from the numerical resolution of Eq. (4) in $Fe_{0.81}Cr_{0.19}$ at $T = 773K$. As $f(c)$ is isotropic, this profile is a function of radial position $r = ||\mathbf{x}||$ only. This concentration profile does not level off toward the center of the precipitate and cannot be approximated by a hyperbolic tangent function as in the case of liquid–gas transitions.[37] This may explain the convergence difficulties the CSDD and GAD methods encounter, since hyperbolic tangent functions are often used as initial conditions in these methods.[22,38] It is apparent that the chromium concentration at the center of the precipitate ($c(0) \approx 0.56$), differs substantially from the solubility limit of the bulk of the new Cr-rich phase, c_β at this temperature, as CNT postulates. At large r values, the atomic fraction of the metastable phase, $\bar{c} = 0.19$ is recovered. The inset in Fig. 1 shows the eigenvector $v_0(r)$ associated with the unique negative eigenvalue of $\frac{\delta^2\Omega[c]}{\delta c^2}$ at the saddle point. This vector is also largely different from $v_0(r)$ computed in the case of liquid-gas transitions.[37] We have verified that the eigenvalue of $\frac{\delta^2\Omega[c(r)]}{\delta c(r)^2}$ associated with $v_0(r)$, i.e., in the presence of critical precipitates, is its only negative eigenvalue, thus demonstrating that the index of the saddle point is 1. To demonstrate the unstable nature of the chromium distribution at the saddle point, the time evolution of different concentration profiles $c(r) \pm \varepsilon v_0(r)$ was obtained from solving the CH equation. The results of these computations are also illustrated in Fig. 1. The profile either converges to a concentration distribution such that the maximum Cr concentration is equal to c_β, as prescribed by the equilibrium phase diagram (brown and blue dashed lines in Fig. 1) or spreads out to reach the uniform value, $\bar{c}$, determined by the initial metastable phase (red and green dashed lines).

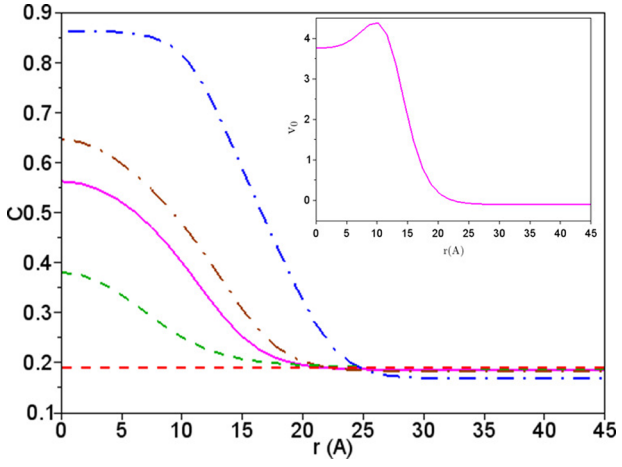

FIG. 1. Concentration profile $c(r)$ for critical precipitates computed from a 3D numerical resolution of Eq. (4) (magenta curve). Computation results obtained from solving the CH equation and assuming the initial concentration profile is only slightly different from the critical one (dashed–dotted green line: t = 250; dashed–dotted red line: t = 500 for $c(r) + \varepsilon v_0(r)$; dashed brown line: t = 250; and dashed blue line: t = 500 for $c(r) - \varepsilon v_0(r)$). The inset displays the eigenvector $v_0(r)$ associated with the unique negative eigenvalue of $\frac{\delta^2\Omega[c(r)]}{\delta c(r)^2}$.

In order to assess the theoretical developments we report, a set of experiments were carried out on several ultra-pure $Fe_{0.81}Cr_{0.19}$ samples. The samples, initially heated at 1000 K, were quenched and subsequently annealed at 773 K over different periods. Atom Probe Tomography (APT)[34,39–41] was used to characterize the chromium distribution. The results showed precipitates first appeared when samples were annealed over time-periods greater than 100 h. At this annealing time, all observed precipitates exhibit the same size justifying that we are dealing with critical precipitates.[42]

Figure 2 shows a comparison between the chromium profile obtained from solving Eq. (4) and determined using APT. The remarkable agreement between theory and experiment vindicates the use of Eq. (4) for computing critical precipitates in solids. Also indicated in the figure, the result is computed from CNT (green curve in Fig. 2) which is inadequate in two respects. First, it predicts that the chromium concentration at the critical precipitates' core is equal to the equilibrium concentration of the new phase. Second, it describes a sharp interface which tallies neither with our calculation nor with our experimental results.

Equation (4) was also solved for different values of $\bar{c}$ and the results of these calculations are shown in the inset in Fig. 2. Close to the solubility limit defined by $\bar{c} = c_\alpha = 0.147$, the critical profile (red line in Fig. 2) displays two distinct plateaus for which chromium concentrations are equal to $c_\alpha = 0.147$ and $c_\beta = 0.857$. Such a profile is similar to what is expected from CNT although in our case, it exhibits a diffuse interface that is practically as broad as the precipitate itself. As $\bar{c}$ approaches the value prescribed by the spinodal curve $c_s = 0.228$, the critical profiles (magenta and blue lines in Fig. 2) bear a resemblance to a Gaussian distribution with a diffuse interface and a maximum chromium concentration which is well below the concentration of the equilibrium Cr-rich phase. The inset clearly illustrates that in a binodal regime and at the earliest stage of the growth process,

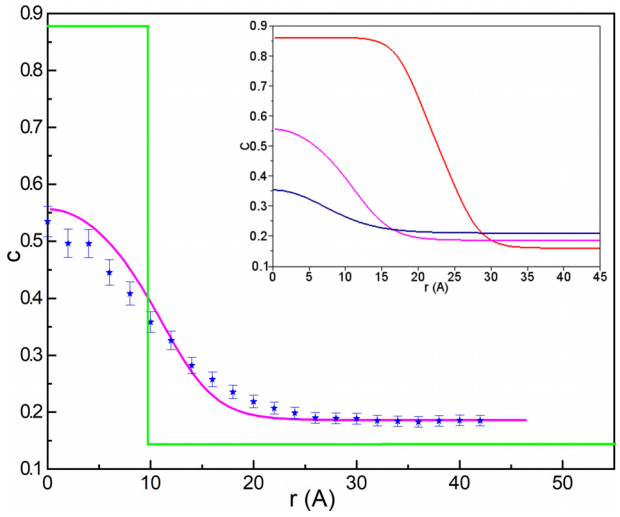

FIG. 2. Comparison between the radial profile (magenta line) computed from Eq. (4) and obtained from APT measurements (blue stars) performed on $Fe_{0.81}Cr_{0.19}$ samples annealed for 100 h at $T = 773K$. The inset shows the chromium concentration calculated from Eq. (4) for different values of $\bar{c}$ within the binodal domain (red curve: $\bar{c} = 0.16$, magenta curve: $\bar{c} = 0.19$, and blue curve: $\bar{c} = 0.21$).

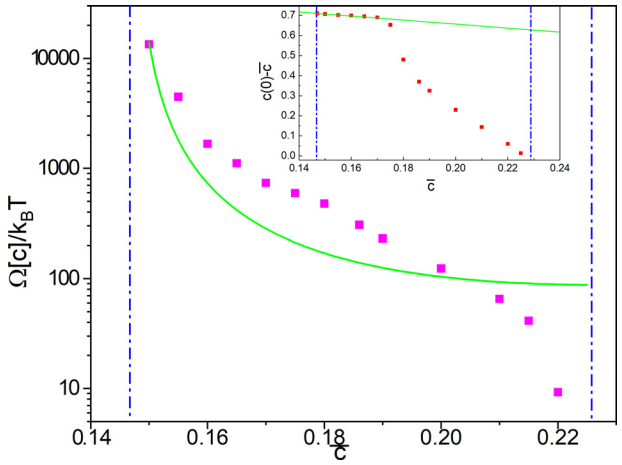

FIG. 3. Comparison between the reduced energy barrier calculated from Eq. (4) (magenta squares) and from CNT (green continuous line) for different values of $\bar{c}$ in the binodal domain. Blue vertical lines represent the limits of the binodal region. The inset shows the comparison between Cr-concentration amplitude across critical precipitates as a function of $\bar{c}$, as calculated from CNT (green line) and from the numerical resolution of Eq. (4) (red squares).

the material may not, in general, be described as consisting of well-defined precipitates of characteristic radii, embedded in a matrix, both of which are of uniform concentration.

Having validated our approach against relevant experimental data now enables us to determine conditions in which other methods may be applied for calculating the characteristics of critical precipitates. Solutions to Eq. (4) were determined for several chromium concentration values in the binodal region, whence the height of the reduced energy barrier $\frac{\Omega[c]}{k_B T}$, (i.e., the energy difference between the grand potential energy at the saddle point and the metastable state) was derived. The corresponding values are shown in Fig. 3 and compared to calculations obtained within CNT. The Cr-concentration amplitude, $c(0) - \bar{c}$, across a Cr-rich critical precipitate as a function of $\bar{c}$ is also shown in the inset in Fig. 3. The figure shows that although the energy barrier and Cr-concentration amplitudes are similar to those obtained from CNT at the solubility limit, substantial discrepancies prevail everywhere else. In particular, in our approach, the energy barrier and the Cr-concentration variations both fall to zero as the composition of the alloy approaches the spinodal limit. This is expected since thermal fluctuations are sufficient in this case to trigger the growth process. By contrast, CNT predicts these quantities are strictly positive at that point. CNT is, therefore, only applicable in the binodal domain for compositions sufficiently close to the binodal limit. Our calculation also enables us to determine the conditions in which the stochastic phase field method may be used. The reduced energy barrier must be lower than 10, in order to apply this method and Fig. 3 shows that this is only true when the alloy composition approaches the spinodal limit. Our experimental data were obtained for average Cr-concentrations of 0.19, a value commonly encountered in engineering applications, and our figure demonstrates that neither CNT nor the stochastic phase field approach are applicable.

This Letter provides a substantial contribution toward solving the outstanding problem of the formation of critical nuclei in nucleation and growth regimes. This is done by setting up a fictitious dynamics,[43] the saddle points of which correspond to that of the free energy functional, and by determining these saddle points, whence critical nuclei characteristics are obtained. The model is backed up against original data we have obtained from ultra-pure $Fe_{0.81}Cr_{0.19}$ samples, using atomic probe tomography. The data provide a measure of the chromium concentration in the vicinity of Cr-rich regions at the very beginning of the growth process and enable a very straightforward comparison to our model. The theory and experiment are shown to tally remarkably well. On the strength of this, we calculate critical precipitate characteristics, for several average Cr-concentration values. This provides a means of establishing the conditions in which it is licit to apply CNT or the stochastic phase field method. The method we have implemented is independent of the form of the free energy. It is, therefore, not restricted to metallurgical applications but may be used in many different fields of physics and chemistry. The main interest of our approach in comparison with the previous approaches is that the critical profile can be obtained from the metastable state. The critical profile then provides the initial condition for the Cahn–Hillard or the Cahn–Allen equations in the binodal regime. Our method should then allow modeling the long time evolution of the microstructure, i.e., the coarsening.

AUTHOR DECLARATIONS

Conflict of Interest

The authors have no conflicts to disclose.

Author Contributions

Laurence Lunéville: Conceptualization (equal). **Philippe Garcia:** Methodology (equal). **Olivier Tissot:** Conceptualization (equal). **David Simeone:** Conceptualization (equal).

DATA AVAILABILITY

The data that support the findings of this study are available from the corresponding author upon reasonable request.

REFERENCES

[1]J. Zhou, Y. Yang, D. Kim, A. Yuan, X. Tian, C. Ophus, and F. Sun, "Observing crystal nucleation in four dimensions using atomic electron tomography," Nature **570**, 500–516 (2019).

[2]K. Kelton and A. Greer, *Nucleation in Condensed Matter: Application in Materials and Biology* (Pergamon, 2010).

[3]D. Porter, K. Easterling, and M. Sherif, *Phase Transformations in Metals and Alloys* (CRC Press, 2009).

[4]M. Jucker and L. Walker, "Self-propagation of pathogenic protein aggregates in neurodegenerative diseases," Nature **501**, 45–51 (2013).

[5]K. R. Gann, C. S. Chang, M.-C. Chang, D. R. Sutherland, A. B. Connolly, D. A. Muller, R. B. van Dover, and M. O. Thompson, "Initial nucleation of metastable γ-Ga_2O_3 during sub-millisecond thermal anneals of amorphous Ga_2O_3," Appl. Phys. Lett. **121**, 062102 (2022).

[6]W. Wohler and T. Schilling, "Hard sphere crystal nucleation rates: Reconciliation of simulation and experiment," Phys. Rev. Lett. **128**, 238001 (2022).

[7]I. S. Winter, R. E. Rudd, T. Oppelstrup, and T. Frolov, "Nucleation of grain boundary phases," Phys. Rev. Lett. **128**, 035701 (2022).

[8]D. Schwarz, R. van Gastel, H. J. Zandvliet, and B. Poelsema, "Size fluctuations of near critical nuclei and Gibbs free energy for nucleation of BDA on Cu(001)," Phys. Rev. Lett. **109**, 016101 (2012).

[9]Y. Zhang, C. Simon, T. Volkmann, M. Kolbe, D. Herlach, and G. Wilde, "Nucleation transitions in undercooled $Cu_{70}Co_{30}$ immiscible alloy," Appl. Phys. Lett. **105**, 041908 (2014).

[10]J. W. Cahn and J. E. Hilliard, "Free energy of a nonuniform system. I. Interfacial free energy," J. Chem. Phys. **28**, 258 (1958).

[11]R. Becker and W. Doring, "Kinetic treatment of nucleation in supersaturated vapors," Ann. Phys. **416**, 719–752 (1935).

[12]Y. B. Zeldovich, "On the theory of new phase formation: Cavitation," Acta Phys. Chem. USSR **18**, 7 (1943).

[13]J. Langer, "Theory of the condensation point," Ann. Phys. **41**, 108 (1967).

[14]D. Gunton, M. San Migel, and P. Sahni, "The dynamics of first order phase transitions," in *Phase Transitions and Critical Phenomena*, edited by C. Domb and J. Lebowitz (Academic Press, 1983), Vol. 8, pp. 269–466.

[15]N. Ghoniem and D. Walgraef, *Instabilities and Self Organization in Materials* (Oxford Science Publications, 2008), Vol. I.

[16]A. G. Khatchaturyan, *Theory of Structural Transformation in Solids* (Wiley Interscience, 1983).

[17]J. W. Cahn and J. E. Hilliard, "Free energy of a nonuniform system. III. Nucleation in a two-component incompressible fluid," J. Chem. Phys. **31**, 688 (1959).

[18]P. W. Bates and P. P. C. Fife, "The dynamics of nucleation for the Cahn–Hilliard equation," SIAM J. Appl. Math. **53**, 990–1008 (1993).

[19]D. Blomker, S. Maier-Paape, and T. Wanner, "Second phase spinodal decomposition for the Cahn–Hilliard–Cook equation," Trans. Am. Math. Soc. **360**, 449–489 (2008).

[20]Q. Bronchart, Y. L. Bouar, and A. Finel, "New coarse-grained derivation of a phase field model for precipitation," Phys. Rev. Lett. **100**, 015702 (2008).

[21]T. Heo, L. Zhang, Q. Du, and L. Chen, "Incorporating diffuse-interface nuclei in phase-field simulations," Scr. Mater. **63**, 8–11 (2010).

[22]Y. Li, S. Hu, L. Zhang, and X. Sun, "Non-classical nuclei and growth kinetics of Cr precipitates in FeCr alloys during ageing," Modell. Simul. Mater. Sci. Eng. **22**, 025002 (2014).

[23]E. Weinan, W. Ren, and E. Vanden-Eijnden, "String method for the study of rare events," Phys. Rev. B **66**, 052301 (2002).

[24]E. Weinan and X. Zhou, "The gentlest ascent dynamics," Nonlinearity **24**, 1831 (2011).

[25]R. S. Maier and D. L. Stein, "Droplet nucleation and domain wall motion in a bounded interval," Phys. Rev. Lett. **87**, 270601 (2001).

[26]L. Zhang, L.-Q. Chen, and Q. Du, "Morphology of critical nuclei in solid-state phase transformations," Phys. Rev. Lett. **98**, 265703 (2007).

[27]F. M. Nyikosa, "Global optimisation using gentlest ascent dynamics and saddle point stability of functions on differentiable manifolds," Ph.D. thesis (Imperial College, 2013).

[28]G. Strang, "The discrete cosine transform," SIAM Rev. **41**, 135–147 (1999).

[29]D. J. Eyre, "Unconditionally gradient stable time marching the Cahn–Hilliard equation," MRS Proc. **529**, 39 (1998).

[30]B. P. Vollmayr-Lee and A. D. Rutenberg, "Fast and accurate coarsening simulation with an unconditionally stable time step," Phys. Rev. E **68**, 066703 (2003).

[31]P. Tolédano and V. Dmitriev, *Reconstructive Phase Transitions: In Crystals and Quasicrystals* (World Scientific, 1996).

[32]A. Jacob, E. Povoden-Karadenzi, and E. Kozeschnik, "Revised thermodynamic description of the Fe–Cr system based on an improved sublattice model of the sigma phase," CALPHAD: Comput. Coupling Phase Diagrams Thermochem. **60**, 16–28 (2018).

[33]W. Xiong, P. Hedstrom, M. Selleby, J. Odqvist, M. Thuvander, and Q. Chen, "An improved thermodynamic modeling of the Fe–Cr system down to zero kelvin coupled with key experiments," CALPHAD: Comput. Coupling Phase Diagrams Thermochem. **35**, 355–366 (2011).

[34]S. Novy, P. Pareige, and C. Pareige, "Atomic scale analysis and phase separation understanding in a thermally aged Fe–20 at.%Cr alloy," J. Nucl. Mater. **384**, 96–102 (2009).

[35]B. Sadigh and P. Erhart, "Calculation of excess free energies of precipitates via direct thermodynamic integration across phase boundaries," Phys. Rev. B **86**, 134204 (2012).

[36]J. Robson, "Modelling the overlap of nucleation, growth and coarsening during precipitation," Acta Mater. **52**, 4669–4676 (2004).

[37]J. Langer, "Theory of spinodal decomposition in alloys," Ann. Phys. **65**, 53 (1971).

[38]J. Zhou, J. Odqvist, J. Ågren, A. Ruban, M. Thuvander, W. Xiong, G. B. Olson, and P. Hedström, "Direct atom probe tomography observations of concentration fluctuation in Fe–Cr solid solution," Scr. Mater. **98**, 13–15 (2015).

[39]M. K. Miller, J. M. Hyde, M. G. Hetherington, A. Cerezo, G. D. W. Smith, and C. M. Elliott, "Spinodal decomposition in Fe–Cr alloys: Experimental study at the atomic level and comparison with computer models—I. Introduction and methodology," Acta Metall. **43**, 3385–3401 (1995).

[40]C. Pareige, M. Roussel, S. Novy, V. Kuksenko, P. Olsson, C. Domain, and P. Pareige, "Kinetic study of phase transformation in a highly concentrated Fe–Cr alloy: Monte Carlo simulation versus experiments," Acta Mater. **59**, 2404–2411 (2011).

[41]O. Tissot, C. Pareige, M.-H. Mathon, M. Roussel, E. Meslin, B. Décamps, and J. Henry, "Comparison between SANS and APT measurements in a thermally aged Fe-19at.%Cr alloy," Mater. Charact. **151**, 332–341 (2019).

[42]L. Lifshitz and V. Sloyzov, "The kinetics of precipitation from supersaturated solid solution," J. Phys. Chem. Solids **19**, 35 (1961).

[43]P. Rabinowitz, *Methods in Critical Point Theory with Application to Differential Equations* (American Mathematical Society, 1986).